ORIGIN AND SIGNIFICANCE OF UPRANGE RAY PATTERNS. P. H. Schultz,[1] J. B. L. Anderson[2], and B. Hermalyn, [1]Brown University, Department of Geological Sciences, 324 Brook Street, Providence, RI 02912-1846 (peter_schultz@brown.edu), [2]Department of Geoscience, Winona State Univ., Winona, MN.

Introduction: Crater rays radiate from fresh primary craters on the Moon, Mercury, and Mars. On the Moon, they are related to secondary craters [1,2,3], scouring of the surface [2], or deposition of distal deposits [2]. On Mars, they also can be shown to be related to secondary craters (e.g., [4,5]) or blast winds [6,7]. Observations of arcuate uprange rays emanating from the Deep Impact collision have been interpreted as an evolving excavation flow field [8] based on laboratory experiments [9]. Here we reconsider the significance of different types of uprange crater ray patterns and provide a simple analytical approximation in order to infer their significance.

Uprange Ray Patterns: Two different crater ray patterns are found on the Moon, Mars, and Mercury: convex (Fig. 1, Fig. 2a) and concave (Fig. 2b). The former has been described as *cardioid* pattern (heart shaped, e.g., [8,10]), whereas the latter is described here as an *arachnid* pattern. Rays extending from secondary craters represent extreme case of the arachnid pattern and form a *horseshoe* (U-shaped) pattern open downrange (e.g., [10]).

Uprange *cardioid* rays occur on the Moon, whether in the highlands or on the smooth plains. The arcuate uprange rays from the 102 km-diameter lunar crater Tycho represent one of the best-known examples. Other notable examples include Proclus, Petavius B, and Stevinus A on the nearside and Jackson (Fig. 1) on the farside. Secondary crater chains comprising these rays generally point back to their primary crater. Crater rays, however, do not necessarily extend back, appearing to miss the crater entirely.

The uprange *arachnid* pattern is best expressed on Mars (Fig. 2b) but was observed at a certain stage in the evolution of the DI impact as well [8]. This pattern appears to be most commonly associated with craters formed in layered targets (low density layer covering basement). Low-thermal inertia distal rays from small craters in THEMIS-night images [e.g., [5] illustrate this pattern. Both cardioid and arachnid patterns can occur around the same crater (Figg. 2b).

Horshoe rays characterize secondary craters around large primaries (>20 km on the Moon). This pattern reflects an absence of uprange material; instead, tertiary ejecta rays wrap around the lead crater or extend obliquely from a cluster [11].

In addition, there are oblique impacts (uprange and downrange zones of avoidance) with radial rays. These are more typically found on Mercury or at small scales (in the regolith).

Origin: Oblique impact experiments into low-density targets at the NASA Ames Vertical Gun Range have produced very similar patterns (Fig. 3). Impacts into nominal sand targets do not clearly produce arcuate uprange ejecta limits, except at very low impact angles (< 10°) or at low (< 1 km/s) speeds. High-speed ejecta (comparable to distal lunar rays) from hypervelocity impacts into sand are lost (except in high speed imaging) but can be mapped in space through reconstruction of their velocities as a function of direction. Three-dimensional particle imaging velocimetry (3D-PIV) now allow tracing this evolution of ejecta in different directions [12] and reveal the uprange zone of avoidance as a function of impact angle. When ejecta particles are tracked as they leave the crater through time, a cardioid pattern emerges [8].

Sych patterns reflect an evolving cratering flow field along the trajectory as the impactor transfers its energy and momentum into the target. This coupling is a three-dimensional process, expressed by evolving ejection angles and ejected mass [10]. Initial coupling at the surface produces low-angle, high-speed ejecta downrange but initially little ejecta uprange. As the crater grows, ejection angles steepen and emerge from greater depths in nearly all directions. While near-rim ejecta asymmetries are subtle in experiments, very low density and compressible targets accentuate arcuate uprange rays that extend back to and across the crater rim [8]. This was as an expression of an asymmetric flow field persisting throughout most of crater growth.

Arachnid patterns also have been produced in laboratory experiments for impacts into layered targets, thereby indicating a change in the flow field with depth. More generally, the different ray patterns from oblique impacts reflect the effect of target/projectile impedance contrasts and the ratio of impactor size divided by its speed.

Discussion: Ray patterns observed in small-scale laboratory experiments and large-scale planetary craters can be connected through scaling relations where the initial coupling depends on the trajectory (non-radial flow) but evolves to conditions limiting crater growth (radial flow). This is illustrated conceptually in Figure 4 but can be described mathematically as an epicycle with one cusp. The radius (velocity vector) increases with azimuth around the center (crater). Close to the crater, the radius center moves along the trajectory with time. Both velocity and degree of asymmetry decrease with time. Far from the crater, however, the source (radius center) appears stationary.

If this interpretation is valid, then arcuate uprange crater rays not only reflect impact angle but also the the projectile-to-crater diameter ratio. At laboratory scales, this ratio for sand is ~ 40 for hypervelocity oblique (30°) impacts. At planetary scales (10's of km), it reduces to 15-20 but will depend on gravity, impactor density (target and projectile), as well as projectile speed. For gravity-controlled craters of the same size, the size of the impactor (65 km/s) producing a crater on Mercury will be ~60% smaller than the same-size crater on the Moon (23 km/s). For retrograde comets impacting Mercury, the projectile will be two times smaller for the same size crater on the Moon. On Mars (12 km/s), however, the projectiles should be ~45% larger. Consequently, the uprange ray pattern may provide clues to impactor type (comet versus asteroidal) for oblique impacts. Retrograde comets may have linear rays even though oblique (zones of uprange avoidance), whereas prograde asteroids will have accentuated cardioid rays. Oblique impact crater on Mars should be characterized by the uprange cardioid pattern due to lower impact speeds. Low-density surface materials (e.g., aeolian loess), however, should result in arachnid ray patterns (Fig. 2b).

Consequently, arcuate ray patterns provide new clues to the early-time cratering flow field and can be inverted to provide conditions of impact.

[1] Oberbeck, V. R. *et al*. (1974) Proc. Lunar Sci. Conf-, Sth, p. 111-136; [2] Schultz, P. H. (1976), Moon Morphology, U. Texas press, 628pp; [3] Hawke, B. R. et al. (2004), *Icarus 170*, 1-16; [4] McEwen A. S., *et al*. (2005), *Icarus* 176, 351-381; [5] Tornabene, L. L., *et al*. (2006), *J. Geophys. Res.* 111(E10), CiteID E10006; [6] Schultz P.H. (1988), *Lunar and Planet. Sci. XIX*, LPI, Houston, pp. 1039-1040; [7] Wrobel, K. *et al*. (2006), *MAPS*, 41, Issue 10, p.1539-1550; [8] Schultz, P. H., *et al*., (2007), *Icarus 190*, 295-333; [9] Herrick, R. *et al*. (2008), *LPSC 38*, No. 1391; [10] Anderson, J. L. B. and Schultz, P. H. (2006), *LPSC 37*, abstract no.1726; [11] Schultz P.H. and Gault D.E. (1984), *J. Geophys. Res. 90,* pp. 3701-3732; [12] Anderson, J. L. B. *et al*. (2003), *MAPS 39*, 303-320.

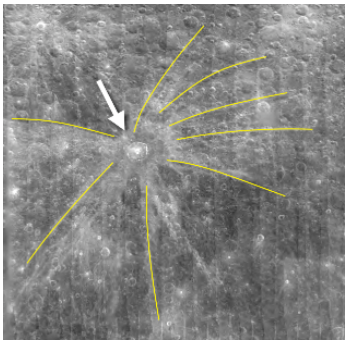

Figure 1: Farside lunar crater Jackson (71 km diameter) exhibiting distinctive cardioid uprange ray system similar to Tycho.

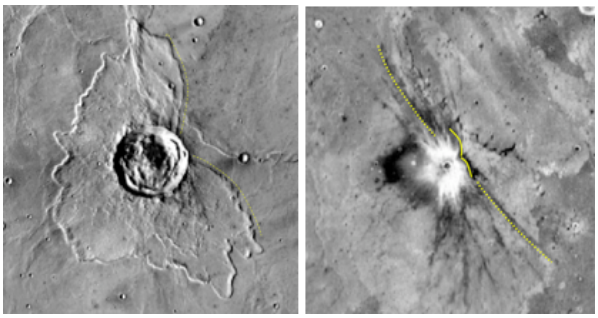

Figure 2: Oblique impact craters on Mars illustrating cardioid-shaped uprange (left) and composite crater, Dilly (right). The similarity with other ballistic ray patterns indicates for a curtain-driven vortex origin for the terminal ramparts. The small crater Dilly (2 km diameter) exhibits a low-thermal inertia (dark) distal arachnid ray pattern and a high-thermal inertia proximal rim deposits. This suggests a low-density surface layer.

Figure 3: Example of cardioid shaped ray pattern uprange for an oblique hypervelocity impact (~ 5 km/s) into low density sieved perlite. In this case, the impact point is on the uprange wall.

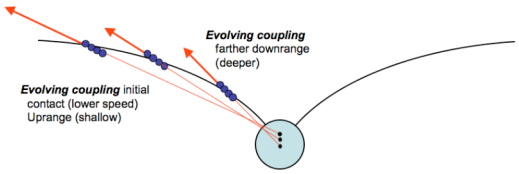

Figure 4: Conceptual depiction for origin of cardioid ray pattern that maps the migration of the flow-field center during excavation.

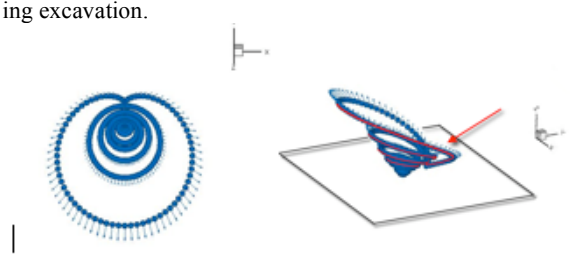

Figure 5: Evolution of in-flight ejecta at 160 ms after impact viewed from above (slightly uprange (left) and from the side (right). This captures highest speed ejecta that will form the cardioid (heart-shaped) distal rays.